Single Reconstituted Neuronal SNARE Complexes Zipper in Three Distinct Stages

Ying Gao *et al.*

Science **337**, 1340 (2012);
DOI: 10.1126/science.1224492

Science (print ISSN 0036-8075; online ISSN 1095-9203) is published weekly, except the last week in December, by the American Association for the Advancement of Science, 1200 New York Avenue NW, Washington, DC 20005.

20. Y. Koide *et al.*, *Genetics* **180**, 409 (2008).
21. L. Wang *et al.*, *Plant J.* **61**, 752 (2010).
22. H. Yoshida *et al.*, *Dev. Cell* **4**, 265 (2003).
23. Y. Oono *et al.*, *Plant Biotechnol. J.* **8**, 691 (2010).
24. Y. Wakasa *et al.*, *Plant J.* **65**, 675 (2011).
25. S. Hayashi, Y. Wakasa, H. Takahashi, T. Kawakatsu, F. Takaiwa, *Plant J.* **69**, 946 (2012).
26. N. Watanabe, E. Lam, *J. Biol. Chem.* **283**, 3200 (2008).
27. H. Matsumura *et al.*, *Plant J.* **33**, 425 (2003).
28. R. Blanvillain *et al.*, *EMBO J.* **30**, 1173 (2011).
29. D. Pontier, M. Tronchet, P. Rogowsky, E. Lam, D. Roby, *Mol. Plant Microbe Interact.* **11**, 544 (1998).
30. S. Lee, K.-H. Jung, G. An, Y.-Y. Chung, *Plant Mol. Biol.* **54**, 755 (2004).
31. H. Li *et al.*, *Plant Physiol.* **156**, 615 (2011).
32. H. Du, Y. Ouyang, C. Zhang, Q. Zhang, *New Phytol.* **191**, 275 (2011).

Acknowledgments: We thank D. S. Brar of the International Rice Research Institute for providing the rice seeds, and S. Luan of University of California, Berkeley, USA for discussion. This research was supported by grants from the National Natural Science Foundation (31130032 and 30921091), the 863 Project (2012AA100103), and the 111 Project (B07041) of China. All of the DNA sequences obtained in this study have been deposited in the GenBank from accession codes JX138498 to JX138505. A patent for the ORF5 sequence has been approved by the State Intellectual Property Office of China (ZL200710053552.9).

Supplementary Materials

www.sciencemag.org/cgi/content/full/337/6100/1336/DC1
Materials and Methods
Figs. S1 to S10
Tables S1 to S7
References (*33*–*41*)

23 April 2012; accepted 13 June 2012
10.1126/science.1223702

Single Reconstituted Neuronal SNARE Complexes Zipper in Three Distinct Stages

Ying Gao, Sylvain Zorman, Gregory Gundersen, Zhiqun Xi, Lu Ma, George Sirinakis, James E. Rothman,* Yongli Zhang*

Soluble *N*-ethylmaleimide–sensitive factor attachment protein receptor (SNARE) proteins drive membrane fusion by assembling into a four-helix bundle in a zippering process. Here, we used optical tweezers to observe in a cell-free reconstitution experiment in real time a long-sought SNARE assembly intermediate in which only the membrane-distal amino-terminal half of the bundle is assembled. Our findings support the zippering hypothesis, but suggest that zippering proceeds through three sequential binary switches, not continuously, in the amino- and carboxyl-terminal halves of the bundle and the linker domain. The half-zippered intermediate was stabilized by externally applied force that mimicked the repulsion between apposed membranes being forced to fuse. This intermediate then rapidly and forcefully zippered, delivering free energy of 36 k_BT (where k_B is Boltzmann's constant and T is temperature) to mediate fusion.

Soluble *N*-ethylmaleimide–sensitive factor attachment protein receptor (SNARE) proteins mediate membrane fusion in the cell, and in particular the fusion of vesicles stored at nerve endings to release neurotransmitters for synaptic transmission (*1*, *2*). The neuronal SNAREs consist of vesicle-associated membrane protein 2 (VAMP2, also called synaptobrevin) on the vesicle membrane (v-SNARE) and the binary complex of syntaxin 1 and SNAP-25 on the plasma membrane (target or t-SNARE) (*3*, *4*). Together these SNAREs drive membrane fusion by joining into a parallel four-helix bundle (*4*), which is envisioned to zipper progressively toward the membranes (*5*), providing force that overcomes an estimated energy barrier of >40 k_BT (where k_B is Boltzmann's constant and T is temperature) (*6*). Considerable indirect evidence favors the zippering hypothesis (*7*–*12*), but direct observation of the assembly intermediates and accurate characterization of the zippering energy and kinetics have been lacking.

We developed a single-molecule manipulation assay to investigate SNARE assembly based on high-resolution dual-trap optical tweezers (Fig. 1A). We cross-linked the N termini of syntaxin and VAMP2 by a disulfide bridge and attached syntaxin by its C terminus to one bead and VAMP2 to another through a DNA handle (*13*). The experiment was started with a single preassembled SNARE complex containing truncated syntaxin (187–265) and VAMP2 (25–92) and full-length SNAP-25 (*4*, *14*) to avoid misassembled SNARE by-products (*10*, *15*).

The protein-DNA conjugate extended with the increasing pulling force in a nonlinear manner predicated by the worm-like chain model (Fig. 1B and fig. S2). However, the monotonic force and extension curves were interrupted by abrupt changes caused by SNARE disassembly or reassembly (Fig. 1C). Fast reversible transitions appeared in two force regions, the first in the range of 8 to 13 pN with ~3-nm average extension change (Fig. 1D and fig. S3) and the second in the range of 14 to 19 pN with ~7-nm extension change (Fig. 1D and fig. S4). Both transitions occurred between two states (fig. S5 and table S1), manifesting two distinct binary switches in SNAREs. When the linker domain (LD) of VAMP2 was deleted, the first transition disappeared, whereas the second transition remained (fig. S6). Thus, the first transition is caused by reversible folding and unfolding of the LD alone. The average size of the extension change suggests that a total of 22 (±3, SD) amino acids or 10 amino acids in VAMP2 (83–92) participated in the transition (fig. S7A). This observation is consistent with a fully zippered LD in a coiled-coil conformation in solution (Fig. 1B, state 1) as seen in the crystal structure of the SNARE complex (*4*, *16*). Further deletion into the C-terminal SNARE domain of VAMP2 (Vc) abolished the second transition (fig. S8), which suggests that this VAMP2 region is involved in the transition.

The additional ~7-nm extension increase from the LD unfolded state (Fig. 1B, state 2) leads to a partially zippered SNARE state (state 3, Fig. 1E). To derive the structure, energy, and kinetics associated with this state, we measured the real-time transition involving Vc at different mean forces (Fig. 1D). The fast two-state transition was confirmed by hidden-Markov modeling (HMM) (*17*) and the histogram distribution of extension (figs. S5B and S9). On the basis of the measured extension change and an asymmetrical transition model (fig. S10) (*18*), we found that 26 (±3) amino acids in VAMP2 (57–82) were unzipped in the partial SNARE complex (Fig. 1E). This places the interface of the unzipped Vc and the zippered N-terminal VAMP2 (Vn) at residue 56 (±5, SD; ±1, SEM) or at the central ionic layer of the bundle. This ionic layer is one of the most evolutionarily conserved features of all SNAREs (*19*), yet with unclear functions. Thus, our result suggests a possible role of the ionic layer in stabilizing the half-zippered neuronal SNARE structure crucial for regulation of membrane fusion (*7*, *8*, *12*, *18*, *20*).

The half unfolding probability of Vc (Fig. 2A) determines an average equilibrium force (f_{eq}) of 17 (±2 SD, n = 76) pN, which can be defined as the maximum force output of Vc zippering averaged over the accompanying extension change. This force is the highest equilibrium force reported for any coiled-coil proteins (*17*), including the designed strongest known coiled coil designated as pIL with an equilibrium force of 12.4 pN (*21*). The unfolding probability could be extrapolated to zero force (*14*, *17*, *22*) to reveal the Vc zippering free energy of 28 (±3) k_BT, higher than the folding energy of pIL [24 (±1) k_BT] despite pIL's greater length (33 amino acids) (*21*).

The average Vc zippering rate at the maximum force output (~160 s^{-1}) (Fig. 2B) is also greater than the equilibrium rate of pIL (~10 s^{-1}) (*21*). Yet the rate is much less than the estimated

Department of Cell Biology, Yale University School of Medicine, 333 Cedar Street, New Haven, CT 06520, USA.

*To whom correspondence should be addressed. E-mail: yongli.zhang@yale.edu (Y.Z.); james.rothman@yale.edu (J.E.R.)

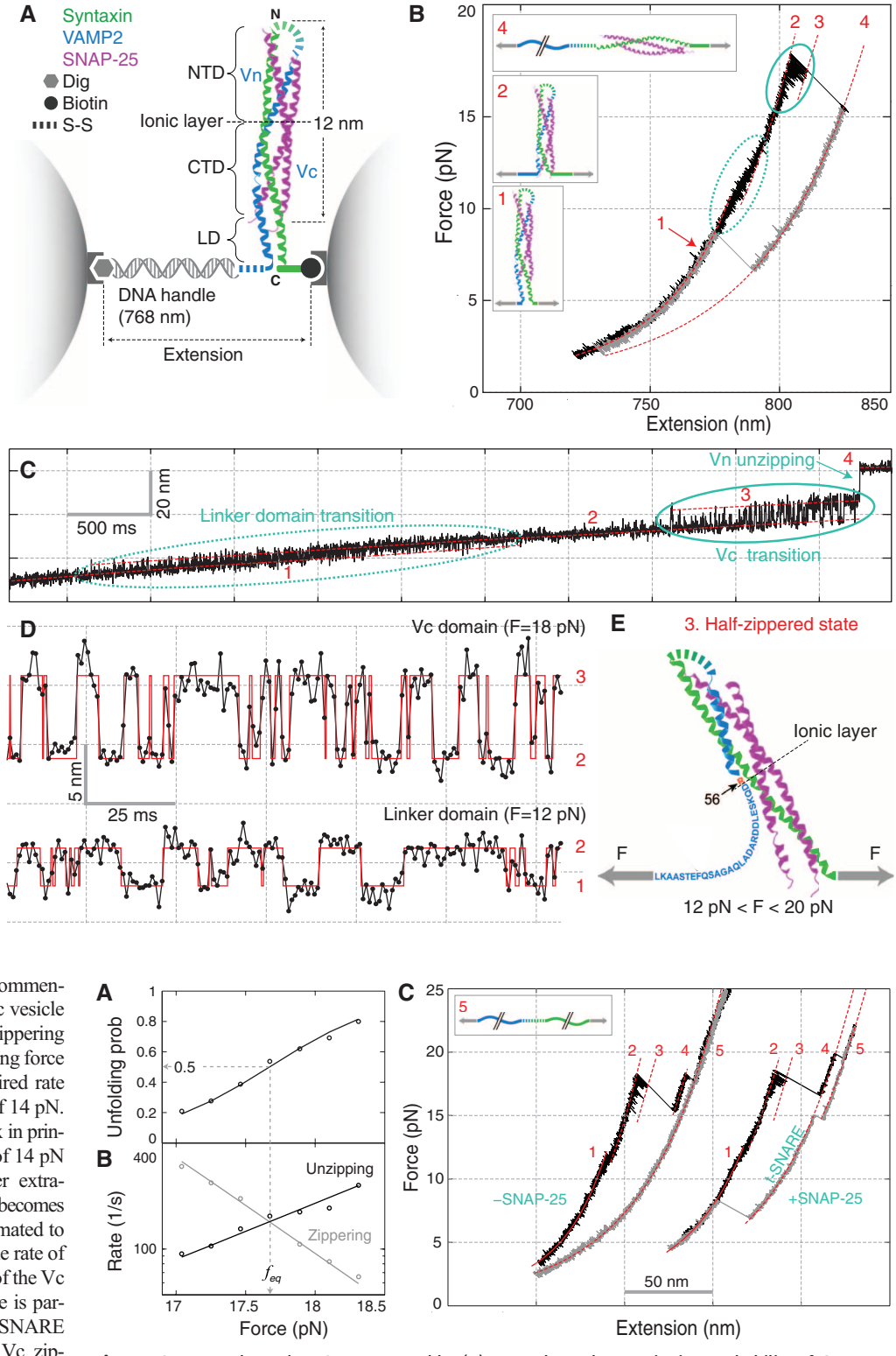

Fig. 1. Dynamic disassembly and reassembly of the single SNARE complex. (**A**) Experimental setup. The SNARE complex contains the N-terminal (NTD) and C-terminal (CTD) SNARE domains, with the corresponding VAMP2 regions designed as Vn and Vc, respectively, separated by the ionic layer and the linker domain (LD). (**B**) Force-extension curve (FEC) of the SNARE-DNA conjugate. The FEC corresponds to the first of five cycles of pull (black) and relaxation (gray) shown in fig. S2. Different segments of the FEC can be fit by the worm-like chain model (red dashed lines), revealing the structures of SNARE assembly states (inset, same red numbering throughout the figures). The LD and CTD transitions are marked by dashed and solid ovals, respectively. (**C**) Time-dependent extension corresponding to the pulling phase from 8.6 to 17.5 pN (fig. S3). (**D**) Extension transitions of LD (bottom) and CTD (top) with their idealized transitions determined by the HMM analysis (red traces). The histogram distributions of extension are shown in fig. S5. (**E**) Structural model of the force-dependent half-zippered state with Vc unzipped to the ionic layer (red).

SNARE zippering rate of 4×10^4 s^{-1} commensurate with the time required for synaptic vesicle fusion (~60 μs) (*23*). However, the Vc zippering rate increases exponentially as the opposing force drops (Fig. 2B) (*17*), reaching the required rate for synaptic fusion at a predicted force of 14 pN. This means that a single SNARE complex in principle can generate a high average force of 14 pN during membrane fusion. When further extrapolated to zero force (*14*), the Vc zippering becomes downhill and barrierless, with a rate estimated to be ~1×10^6 s^{-1} (*21*), corresponding to the rate of the coil-to-helix transition and diffusion of the Vc polypeptide (*24*). This fast zippering rate is partially attributed to the largely ordered t-SNARE complex that serves as a template for Vc zippering (figs. S10 and S11) (*18*). In conclusion, the extraordinarily high force output, energy, and rate qualify Vc zippering as the major power stroke for the fast synaptic fusion (*11*).

Similarly, we measured a folding energy of 8 (±2) k_BT for LD (fig. S7, B and C) with a maximum force output close to that of pIL (~12 pN). An energy barrier of 5 (±2) k_BT was derived, corresponding to a zipping rate of 7×10^3 (9×10^2 to 5×10^4) s^{-1} at zero force. LD also strongly and rapidly zippers, which may transduce and augment the Vc zippering energy to drive membrane fusion. LD's zippering rate and energy may be increased by transmembrane domains (*25*) and proteins such as synaptotagmin and Munc18-1 (*3*, *26*).

The Vc transition generally ended with an irreversible extension jump of 15 (±1) nm (Fig. 1,

Fig. 2. SNAP-25-dependent SNARE assembly. (**A**) Force-dependent unzipping probability of CTD measured on a single SNARE complex. (**B**) Corresponding CTD transition rates. Theoretical predictions are shown in lines. (**C**) FECs measured in the absence (–SNAP-25) and presence (+SNAP-25) of SNAP-25 in solution.

B and C, from states 3 to 4), corresponding to complete Vn unzipping (fig. S12). When immediately relaxed, the SNARE complex first followed a different force-extension curve (FEC) to reach lower force (Fig. 1B). As the force was lowered to 3 to 10 pN, the complex fully and cooperatively reassembled.

The dynamic disassembly and reassembly of a single SNARE complex could be repeated for many cycles of pull and relaxation (fig. S2). However, when the t-SNARE complex was pulled to a higher force (in the range of 15 to 28 pN), one additional irreversible extension jump was observed (Fig. 2C, from states 4 to 5, and fig. S11). No more transitions were seen when further pulling to even higher forces (>30 pN), indicating complete unfolding of the SNARE complex (state 5). Thus, this jump may correspond to unfolding of the remaining t-SNARE complex. When relaxed to low forces (<3 pN), a majority (~85%) of syntaxin and VAMP2 conjugates could not reassemble (Fig. 2C and fig. S2), suggesting dissociation of the SNAP-25 molecule.

To further test the dependence of SNARE assembly on SNAP-25, we repeated the above experiment by adding SNAP-25 in the solution. Single SNARE complexes were fully disassembled by being pulled to high forces and then relaxed to detect SNARE reassembly. At 0.2 μM SNAP-25, the ternary SNARE complex could reassemble at a low force (3 to 10 pN) with a probability of ~0.8 for each round of relaxation (Fig. 2C). This reassembly was always followed by formation of the t-SNARE complex in a higher force range (>12 pN). The SNAP-25 molecule in solution could bind to the syntaxin-VAMP2 conjugate and initiate de novo SNARE assembly. Comparing this to the experiment in the absence of SNAP-25 suggests that the binary t-SNARE is required for SNARE zippering (*27*). In contrast, the affinity between syntaxin and VAMP2 in the absence of SNAP-25 is minimal and could not be detected in our experiments (Fig. 2C) (*10*, *28*).

The assembly and disassembly of the N-terminal domain (NTD) occurred with a large force hysteresis, indicating a large energy barrier for NTD transitions and preventing us from measuring its association energy. To gain insight into NTD's assembly mechanism, we pulled a single SNARE complex from the N-termini of syntaxin and VAMP2 (Fig. 3A) (*14*). The SNARE complex unzipped into t- and v-SNAREs (from states 1′ to 3′) in two parallel pathways. About two-thirds of the 53 complexes tested showed one-step unzipping (FECs i and iii), whereas other complexes exhibited two-step unzipping via a transient intermediate state (state 2′). Reversible transitions were often observed between this state and the fully zippered state 1′ (Fig. 3B) and lasted long enough for the equilibrium transition force and the average extension change to be determined. This partially zippered SNARE complex had Vn unzipped to residue 57 (±3, SEM), or approximately the ionic layer. The Vn domain unzipped at a higher average equilibrium force of 18.5 (±0.4, SEM) pN than Vc from C-terminal pull at 16.7 (±0.2, SEM) pN. In addition, the average extension change of Vn (8.3 ± 0.2, SEM, nm) was greater than that of Vc (7.1 ± 0.1, SEM, nm). These measurements allow an estimation of the folding free energy of 35 (±4) k_BT for NTD assembly in the presence of the preassembled C-terminal domain (CTD) (*14*, *17*). However, Vn assembled much more slowly than Vc (Fig. 3B).

The t-SNARE complex again remained intact after VAMP2 was pulled out (Fig. 3, state 3′). This complex has a structure similar to those obtained from the C-terminal pull (table S1). On average, the t-SNARE complex contained 61 (±4) helical amino acids in the syntaxin molecule, suggesting an approximately fully assembled three-helix bundle for the t-SNARE (figs. S10 and S11). Upon relaxation, the ternary complex could reassemble at an average force of 3.2 (±0.2, SEM) pN (Fig. 3, FEC i), compared to 5.0 (±0.2, SEM) pN from the C-terminal pull. The more force-sensitive assembly of the SNARE complex from the N-terminal pull indicates that initiation of the assembly occurs in NTD (*10*, *17*, *29*).

We suggest a model for three-stage neuronal SNARE assembly through sequential zippering of NTD, CTD, and LD (fig. S13). Overall, SNARE assembly outputs free energy of 65 (±6) k_BT (*14*). This energy is much higher than in previous reports (*28*, *30*, *31*), but justified by our equilibrium measurements required for any thermodynamic quantifications (*14*). These measurements lead to the energy landscape of SNARE zippering (Fig. 4). The CTD zippering energy is enriched at its C-terminal end or in VAMP2 (74–82), leading to a higher local force generation (~34 pN) (fig. S8) (*30*).

The half-zippered state appeared to exist only in the force range of 12 to 20 pN. Below this force range, the state collapsed into the four-helix bundle, consistent with its downhill folding at zero force. Thus, SNARE domain zippering became a two-state process limited by the slow NTD assembly (*10*, *28*). Above this range, the half-zippered state completely unzipped. The half-zippered state

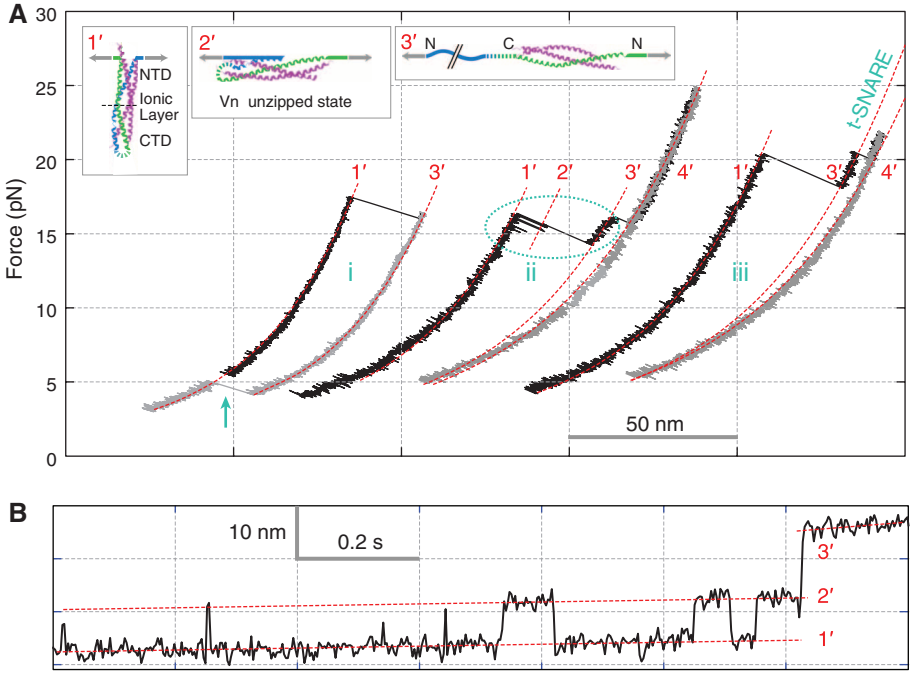

Fig. 3. Disassembly and reassembly of the SNARE complex under N-terminal pulling force. (**A**) FECs and their segmental fit (red dashed line) showing different assembly states (inset) including the completely unfolded state 4′. The full SNARE reassembly (cyan arrow) is t-SNARE dependent. (**B**) Extension-time trace corresponding to the region marked in the dashed oval in (A).

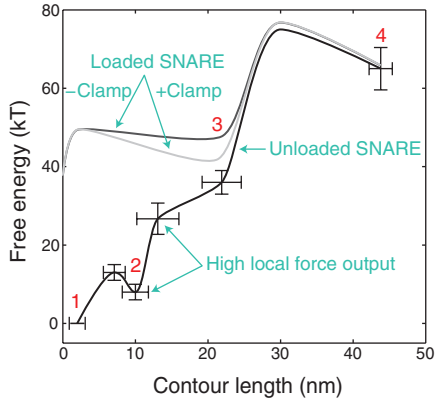

Fig. 4. Sketches of the energy landscapes for SNARE zippering in the absence (black) and presence of the opposing force load from membranes with (light gray) and without (gray) complexin clamp. The contour length of the SNARE complex between the C termini of syntaxin (residue 265) and VAMP2 (residue 92) is chosen as a reaction coordinate. Error bars show the SDs of the measurements.

could be further stabilized by synaptotagmin and complexin (*12*, *18*, *20*) (Fig. 4).

The elegant molecular logic of the SNARE complex thus revealed perfectly fits to precise regulation of neurotransmitter release (*3*), with slow intrinsic assembly of NTD to allow control of vesicle priming by regulatory factors that accelerate NTD assembly, thereby creating the readily releasable pool of neurotransmitters (*11*); an intrinsic pause near the ionic layer stabilized by the repulsion between membranes being forced to fuse to enable clamping by complexin at this stage of zippering (*17*); and unobstructed, fast zippering of CTD and LD to open the fusion pore once the clamp is removed, enabling neurotransmitters to be rapidly released. The pore then expands as the transmembrane domains of VAMP2 and syntaxin dimerize (*32*).

References and Notes

1. T. Söllner *et al.*, *Nature* **362**, 318 (1993).
2. T. Weber *et al.*, *Cell* **92**, 759 (1998).
3. T. C. Südhof, J. E. Rothman, *Science* **323**, 474 (2009).
4. R. B. Sutton, D. Fasshauer, R. Jahn, A. T. Brunger, *Nature* **395**, 347 (1998).
5. P. I. Hanson, R. Roth, H. Morisaki, R. Jahn, J. E. Heuser, *Cell* **90**, 523 (1997).
6. F. S. Cohen, G. B. Melikyan, *J. Membr. Biol.* **199**, 1 (2004).
7. T. Xu *et al.*, *Cell* **99**, 713 (1999).
8. S. Y. Hua, M. P. Charlton, *Nat. Neurosci.* **2**, 1078 (1999).
9. T. J. Melia *et al.*, *J. Cell Biol.* **158**, 929 (2002).
10. A. V. Pobbati, A. Stein, D. Fasshauer, *Science* **313**, 673 (2006).
11. A. M. Walter, K. Wiederhold, D. Bruns, D. Fasshauer, J. B. Sørensen, *J. Cell Biol.* **188**, 401 (2010).
12. M. Kyoung *et al.*, *Proc. Natl. Acad. Sci. U.S.A.* **108**, E304 (2011).
13. C. Cecconi, E. A. Shank, C. Bustamante, S. Marqusee, *Science* **309**, 2057 (2005).
14. Materials and methods in the supplementary materials.
15. K. Weninger, M. E. Bowen, S. Chu, A. T. Brunger, *Proc. Natl. Acad. Sci. U.S.A.* **100**, 14800 (2003).
16. A. Stein, G. Weber, M. C. Wahl, R. Jahn, *Nature* **460**, 525 (2009).
17. Y. Gao, G. Sirinakis, Y. L. Zhang, *J. Am. Chem. Soc.* **133**, 12749 (2011).
18. D. Kümmel *et al.*, *Nat. Struct. Mol. Biol.* **18**, 927 (2011).
19. D. Fasshauer, R. B. Sutton, A. T. Brunger, R. Jahn, *Proc. Natl. Acad. Sci. U.S.A.* **95**, 15781 (1998).
20. F. Li *et al.*, *Nat. Struct. Mol. Biol.* **18**, 941 (2011).
21. Z. Q. Xi, Y. Gao, G. Sirinakis, H. L. Guo, Y. L. Zhang, *Proc. Natl. Acad. Sci. U.S.A.* **109**, 5711 (2012).
22. M. T. Woodside *et al.*, *Science* **314**, 1001 (2006).
23. B. L. Sabatini, W. G. Regehr, *Nature* **384**, 170 (1996).
24. J. Kubelka, J. Hofrichter, W. A. Eaton, *Curr. Opin. Struct. Biol.* **14**, 76 (2004).
25. J. F. Ellena *et al.*, *Proc. Natl. Acad. Sci. U.S.A.* **106**, 20306 (2009).
26. Y. Xu, L. J. Su, J. Rizo, *Biochemistry* **49**, 1568 (2010).
27. E. Karatekin *et al.*, *Proc. Natl. Acad. Sci. U.S.A.* **107**, 3517 (2010).
28. K. Wiederhold, D. Fasshauer, *J. Biol. Chem.* **284**, 13143 (2009).
29. K. Weninger, M. E. Bowen, U. B. Choi, S. Chu, A. T. Brunger, *Structure* **16**, 308 (2008).
30. W. Liu, V. Montana, V. Parpura, U. Mohideen, *J. Nanoneurosci.* **1**, 120 (2009).
31. F. Li *et al.*, *Nat. Struct. Mol. Biol.* **14**, 890 (2007).
32. L. Shi *et al.*, *Science* **335**, 1355 (2012).

Acknowledgments: We thank H. Ji and W. Xu for technical assistance and F. Pincet, T. Melia, and E. Karatekin for valuable discussion. This work is supported by NIH grants GM093341 to Y.Z. and DK027044 to J.E.R. Y.Z. designed the experiments; Y.G., S.Z., G.G., Z.X., L.M., and G.S. performed the experiments; Y.Z. and Y.G. analyzed the data; and Y.Z. and J.E.R. wrote the paper. The data and Matlab codes are in the paper and the supplementary materials.

Supplementary Materials

www.sciencemag.org/cgi/content/full/science.1224492/DC1
Materials and Methods
Figs. S1 to S13
Table S1
References (*33*–*68*)

9 May 2012; accepted 7 August 2012
Published online 16 August 2012;
10.1126/science.1224492

Highly Conserved Protective Epitopes on Influenza B Viruses

Cyrille Dreyfus,[1]* Nick S. Laursen,[1,2]* Ted Kwaks,[3] David Zuijdgeest,[3] Reza Khayat,[1] Damian C. Ekiert,[1]† Jeong Hyun Lee,[1] Zoltan Metlagel,[1]‡ Miriam V. Bujny,[3] Mandy Jongeneelen,[3] Remko van der Vlugt,[3] Mohammed Lamrani,[3] Hans J. W. M. Korse,[3] Eric Geelen,[3] Özcan Sahin,[3] Martijn Sieuwerts,[3] Just P. J. Brakenhoff,[3] Ronald Vogels,[3] Olive T. W. Li,[4] Leo L. M. Poon,[4] Malik Peiris,[4] Wouter Koudstaal,[3] Andrew B. Ward,[1] Ian A. Wilson,[1,5]§ Jaap Goudsmit,[3]§ Robert H. E. Friesen[3]

Identification of broadly neutralizing antibodies against influenza A viruses has raised hopes for the development of monoclonal antibody–based immunotherapy and "universal" vaccines for influenza. However, a substantial part of the annual flu burden is caused by two cocirculating, antigenically distinct lineages of influenza B viruses. Here, we report human monoclonal antibodies, CR8033, CR8071, and CR9114, that protect mice against lethal challenge from both lineages. Antibodies CR8033 and CR8071 recognize distinct conserved epitopes in the head region of the influenza B hemagglutinin (HA), whereas CR9114 binds a conserved epitope in the HA stem and protects against lethal challenge with influenza A and B viruses. These antibodies may inform on development of monoclonal antibody–based treatments and a universal flu vaccine for all influenza A and B viruses.

Influenza viruses continue to cause substantial morbidity and mortality worldwide (*1*). Because current vaccines are typically only effective against the specific viral strains used for vaccination and closely related viruses (*2*) and increasing resistance reduces the effectiveness of the available antiviral drugs (*3*), an urgent need remains for innovative new treatments, both prophylactic and therapeutic (*4*). To this end, we and others have previously described human monoclonal antibodies (mAbs) that neutralize a wide spectrum of influenza A viruses by binding to highly conserved epitopes in the stem region of hemagglutinin (HA), the major viral surface glycoprotein (*5*–*9*). To date, influenza B viruses have received less attention, because they are largely restricted to humans and thus lack the large animal reservoirs that are key to the emergence of pandemic influenza A viruses (*10*).

Although the morbidity and mortality rates attributable to influenza B are lower than those for H3N2 viruses, they are higher than those for H1N1 viruses (*11*). Influenza B viruses are classified as a single influenza type, but two antigenically and genetically distinct lineages cocirculate (*12*), represented by the prototype viruses B/Victoria/2/1987 (Victoria lineage) and B/Yamagata/16/1988 (Yamagata lineage) (*13*). Vaccine manufacturers have therefore recently initiated clinical evaluation of quadrivalent vaccines that include strains from each influenza B lineage, H1N1, and H3N2 (*14*). Given that influenza B viruses are the major cause of seasonal influenza epidemics every 2 to 4 years leading to substantial absenteeism, hospitalization, and death (*11*), mAbs with broad neutralizing activity (bnAbs) against influenza B viruses have important clinical potential.

Combinatorial display libraries, constructed from human B cells of volunteers recently vaccinated with the seasonal influenza vaccine (*9*), were panned by using soluble recombinant HA from various influenza A and B viruses, and phages were subsequently screened for binding to HAs

[1]Department of Molecular Biology, The Scripps Research Institute, 10550 North Torrey Pines Road, La Jolla, CA 92037, USA. [2]Department of Molecular Biology, Gustav Wieds Vej 10C, Aarhus 8000, Denmark. [3]Crucell Vaccine Institute, Janssen Center of Excellence for Immunoprophylaxis, Archimedesweg 4-6, 2301 CA Leiden, Netherlands. [4]State Key Laboratory of Emerging Infectious Diseases and School of Public Health, Li Ka Shing Faculty of Medicine, The University of Hong Kong, 21 Sassoon Road, Pokfulam, Hong Kong, China. [5]Skaggs Institute for Chemical Biology, The Scripps Research Institute, 10550 North Torrey Pines Road, La Jolla, CA 92037, USA.

*These authors contributed equally to this work.
†Present address: Department of Microbiology and Immunology, University of California—San Francisco, 600 16th Street, San Francisco, CA 94143, USA.
‡Present address: Lawrence Berkeley National Laboratory, Department of Bioenergy/GTL and Structural Biology, Berkeley, CA 94720, USA.
§To whom correspondence should be addressed. E-mail: wilson@scripps.edu (I.A.W.); jaap.goudsmit@crucell.com (J.G.)